Environment effects on the Raman spectra of individual single-wall carbon nanotubes: Suspended and grown on polycrystalline silicon

Hyungbin Son
Department of Electrical Engineering and Computer Science, Massachusetts Institute of Technology, Cambridge, Massachusetts 02139-4307

Yuki Hori
Department of Materials Science and Engineering, Massachusetts Institute of Technology, Cambridge, Massachusetts 02139-4307

S. G. Chou
Department of Chemistry, Massachusetts Institute of Technology, Cambridge, Massachusetts 02139-4307

D. Nezich
Department of Physics, Massachusetts Institute of Technology, Cambridge, Massachusetts 02139-4307

Ge. G. Samsonidze
Department of Electrical Engineering and Computer Science, Massachusetts Institute of Technology, Cambridge, Massachusetts 02139-4307

G. Dresselhaus
Francis Bitter Magnet Laboratory, Massachusetts Institute of Technology, Cambridge, Massachusetts 02139-4307

M. S. Dresselhaus[a)]
Department of Physics and Department of Electrical Engineering and Computer Science, Massachusetts Institute of Technology, Cambridge, Massachusetts 02139-4307

Eduardo B. Barros
Departmento de Física, Universidade Federal do Ceará, Fortaleza, CE, 30123-970 Brazil

(Received 9 July 2004; accepted 14 September 2004)

An enhanced Raman signal is observed from individual suspended single-wall carbon nanotubes (SWNTs) and from isolated SWNTs grown on an *n*-doped polycrystalline silicon film used in standard silicon processing. The radial breathing modes of the Raman spectra taken from suspended SWNTs exhibit narrow linewidths, which indicate a relatively unperturbed environment for suspended SWNTs. Clear Raman signals from intermediate frequency modes in the frequency range from 520 to 1200 cm^{-1} are presented, which might allow a detailed study of the phonon band structure of individual SWNTs. © *2004 American Institute of Physics*. [DOI: 10.1063/1.1818739]

Isolated suspended single-wall carbon nanotubes (SWNTs), by virtue of their unperturbed environment, have already provided unique opportunities for furthering our understanding of SWNT properties, such as greatly enhanced transport signals[1] and strong band-gap photoluminescence (PL).[2] In this work, we show that the suspended SWNTs also offer unique opportunities for Raman scattering studies, including enhanced Raman signals, decreased linewidths of the radial breathing modes (RBMs) and the observation of intermediate frequency modes (IFMs) at a single nanotube level.

Recently, the effects of the environment [such as the wrapping of SWNTs with sodium dodecyl sulfate (SDS)[3] and deoxyribonucleic acid (DNA)][4] and of the substrate on the optical properties of SWNTs (such as PL[2–4] and resonance Raman spectroscopy results),[4–7] have been studied in some detail. The optical spectra give information on both the electronic transition energies E_{ii} and the phonon band structure and their dependence on the environment. For example, the PL spectra taken from both SDS-wrapped SWNTs and suspended SWNTs show that the E_{ii} of SDS-wrapped SWNTs are shifted when compared to suspended SWNTs, while the RBM frequencies ω_{RBM} are less affected.[8] However, previously reported works are limited to ensembles of SWNTs.

This work presents the Raman spectroscopic study both of individual suspended SWNTs, which minimize environmental effects, and of individual SWNTs on a heavily *n*-doped polycrystalline silicon (poly-Si) substrate. Both of these studied environments, as is discussed below, also offer special research opportunities.

The suspended SWNTs are grown across two poly-Si electrodes, which serve both as electrical contacts and as elevated structures for suspending the SWNTs. The poly-Si electrodes are fabricated using standard silicon technology [see Fig. 1(a)]. First, a 1 μm thick poly-Si film is grown by chemical vapor deposition (CVD) on top of a thermally grown 1 μm thick SiO_2 film on a silicon substrate. Then, photolithography and a reactive ion etch are used to pattern the poly-Si film and the oxide film.

The electrodes have two regions: the narrow trench region (1–4 μm wide) and the wide trench region (10 μm wide) [see Fig. 1(b)]. During the SWNT growth, a high electric field on the order of 10^6 V/m can be selectively applied

[a)]Author to whom correspondence should be addressed; electronic mail: millie@mgm.mit.edu

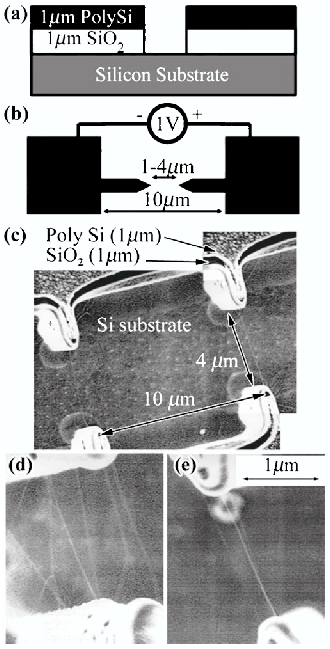

FIG. 1. The electrode structure and SWNTs grown on the electrodes. The schematic of (a) the side view and (b) the top view of the electrode structure. SEM images of (c) the electrode structure, (d) HD suspended SWNTs grown without an applied electric field, and (e) LD suspended SWNTs grown with an applied electric field. The magnification is the same for (d) and (e).

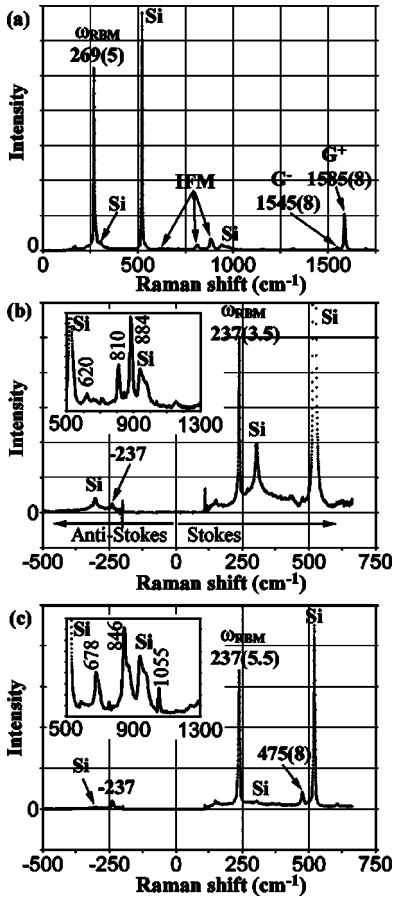

FIG. 2. The Raman spectra taken with $E_{laser}=1.58$ eV from: (a) and (b) individual suspended SWNTs, and (c) an individual SWNT on a poly-Si substrate. The RBM band and G^- band frequencies (FWHM linewidths) are shown. The insets in (b) and (c) are the IFMs taken from an individual suspended SWNT and an individual SWNT on a poly-Si substrate, different from the SWNTs for which the RBM spectra are shown.

across the narrow trenches only. A high electric field is known to enhance the growth rate of SWNTs and to align them.[9,10] Moreover, by controlling the maximum length of the SWNTs, one can guarantee that there are no suspended SWNTs growing across the wide trench, as shown in Fig. 1(c).

The SWNTs are grown directly on the sample by a methane CVD process.[11] Samples were prepared both with and without applied electric fields between the electrodes (see Fig. 1). The iron catalyst nanoparticles are prepared by mixing 50.5 mg of iron(III) nitrate, 21 mg of sodium hydrogen carbonate, and 50 mL of deionized water and stirring the mixture for 1–4 h.[12] To deposit the catalyst particles, the samples are dipped in the catalyst suspension for 1 and 5 min to produce low-density (LD) and high-density (HD) samples, respectively (see Fig. 1). Then, the samples are washed with ethanol and blown dry with nitrogen at room temperature. Finally, the SWNTs were grown at 800–900 °C in the flow of methane (100 sccm), hydrogen (50 sccm), and argon (100 sccm) in a 1 in. tube furnace.

Raman spectra were taken from individual suspended SWNTs and individual SWNTs on a poly-Si substrate using a Raman microprobe laser system in the backscattering geometry and $E_{laser}=1.58$ eV and 2.41 eV laser energy excitation. Figure 2(a) presents a Raman spectrum taken from a suspended SWNT using $E_{laser}=1.58$ eV, where a strong RBM signal, as well as IFMs and relatively narrow G^+ and G^- band spectra [full width at half maximum (FWHM) linewidth $=8$ cm^{-1} for both bands] are observed. The G^- and G^+ mode frequencies are consistent with prior work on the relation between the *A*-symmetry mode frequencies of the G^- and G^+ bands and the ω_{RBM} for individual (n,m) SWNTs.[13] Figures 2(b) and 2(c) show Raman spectra taken from one suspended SWNT and another SWNT on a poly-Si substrate, respectively. For both spectra, we have $\omega_{RBM}=237$ cm^{-1} and both spectra show a particularly low intensity for the anti-Stokes RBM band compared to the Stokes RBM band. Raman signals taken from both kinds of SWNTs are enhanced compared to the Raman signal taken from SWNTs on a Si/SiO_2 substrate for which a signal at $\omega_{RBM}=237$ cm^{-1} (see Fig. 2 of Ref. 5). FWHM RBM linewidths down to 3 cm^{-1} are observed from suspended SWNTs, while RBM linewidths down to 5 cm^{-1} are observed from the SWNTs on a Si/SiO_2 substrate.[14] The RBM bands taken from SWNTs on a poly-Si substrate are usually stronger than the RBM bands taken from suspended SWNTs, and often feature the second harmonic, as shown in Fig. 2(c) at 475 cm^{-1}. These enhanced intensities might be attributed to a surface-enhanced Raman effect from the rough poly-Si surface, where the polycrystalline grain size is about several tens of nanometers. Similar enhanced signals have been reported for SWNTs on rough metal surfaces and on a colloidal silver cluster substrate.[15] The linewidth of the second harmonic is 8 cm^{-1}, which is narrower than the linewidth of the second harmonic of RBM bands reported for SWNT bundles.[16]

The inset figures of Figs. 2(b) and 2(c) show the rich IFM spectra taken from a suspended SWNT and a SWNT on a poly-Si substrate, respectively. IFM spectra were previously observed only in SWNT bundles.[17,18] Due to the enhanced signal, detailed structure in the IFM region can be

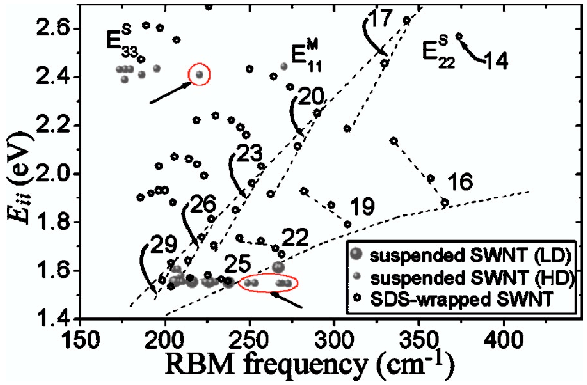

FIG. 3. (Color online) The ω_{RBM} and estimated E_{ii} values obtained experimentally for suspended SWNTs in comparison to SDS-wrapped SWNTs. The dotted lines denote the envelope and the $2n+m$ families for SDS-wrapped semiconducting SWNTs. Points outside the envelope for HD samples are indicated by arrows.

seen. Seven significantly different IFM spectra were observed from four suspended SWNTs and three SWNTs on a poly-Si substrate. The IFMs are related to the phonon band structure and might give information on the chirality of individual SWNTs.[18] Some similar modes have been observed in the IR spectra taken from SWNTs.[19]

The electronic transition energy E_{ii} cannot be determined without a knowledge of the resonance window (ΔE_{res}) or without many excitation laser lines close to each other. However, assuming that ΔE_{res} for suspended SWNTs is equal to or narrower than ΔE_{res} of SWNTs on a Si/SiO_2 substrate, the E_{ii} values can be estimated from the temperature-normalized anti-Stokes-to-Stokes intensity ratio (I_{AS}/I_S) of the RBM bands of the Raman spectra taken from suspended SWNTs.[6] No change in I_{AS}/I_S was found when increasing the laser power up to a maximum power of 20 mW on a 1 μm spot. The temperature was thus assumed to be 300 K. The estimated E_{ii} values and the ω_{RBM} are plotted in Fig. 3 along with the E_{ii} and the ω_{RBM} values obtained from SDS-wrapped SWNTs.[8] The estimated E_{ii} values and the ω_{RBM} taken from the LD samples nearly span the envelope defined by the SDS-wrapped data points, whereas some of the estimated E_{ii} values and the measured ω_{RBM} from the HD samples deviate from the envelope (see Fig. 3). The deviating points might be explained by non-E_{ii} transitions, such as E_{12} or E_{21} transitions, and by similar deviating points previously reported.[20] ω_{RBM} values for the suspended SWNTs match well with those for the SDS-wrapped SWNTs. The errors in E_{ii} are less than ± 0.02 eV for all points. However, there are other sources of errors that are not included: The E_{ii} values for points with $\omega_{\mathrm{RBM}} < 225\ \mathrm{cm}^{-1}$ are not reliable for our setup.[21] The errors in E_{ii} are obtained assuming the resonance window for E_{ii} transitions to be that in Fig. 2 of Ref. 6.

Raman spectroscopy on individual suspended SWNTs opens up a field in SWNT research. Enhanced signals allow a study of normally weak modes, such as IFMs, at the single nanotube level. Narrow linewidths indicate a relatively unperturbed environment, which leaves room for studying the effects of selected perturbations. The substrates might lead to perturbations in the properties of SWNTs, such as their E_{ii} and ω_{RBM} values. These perturbations might allow the study of physics, as in the case of SWNTs on a poly-Si substrate, where enhanced signals for the fundamental RBM and its second harmonic can be observed.

The authors acknowledge support under NSF Grant No. DMR-04-05538. They thank Intel for giving resources to prepare the samples used in this study, and Professor A. Jorio and Professor R. Saito for valuable discussions. This work made use of MR-SEC Shared Facilities supported by the National Science Foundation under Award No. DMR-0213282 and NSF Laser Facility Grant No. CHE-011370. Two of the authors S. G. C. and E. B. B. acknowledge the Dupont-MIT Alliance and CAPES, respectively, for support.

[1] P. Jarillo-Herrero, S. Sapmaz, C. Dekker, L. P. Kouwenhoven, and H. S. J. van der Zant, Nature (London) **429**, 389 (2004).
[2] J. Lefebvre, Y. Homma, and P. Finnie, Phys. Rev. Lett. **90**, 217401 (2003).
[3] S. M. Bachilo, M. S. Strano, C. Kittrell, R. H. Hauge, R. E. Smalley, and R. B. Weisman, Science **298**, 2361 (2002).
[4] S. G. Chou, H. B. Ribeiro, E. Barros, A. P. Santos, D. Nezich, Ge. G. Samsonidze, C. Fantini, M. A. Pimenta, A. Jorio, F. P. Filho, M. S. Dresselhaus, G. Dresselhaus, R. Saito, M. Zheng, G. B. Onoa, E. D. Semke, A. K. Swan, M. S. Ünlü, and B. B. Goldberg, Chem. Phys. Lett. **397**, 296 (2004).
[5] A. Jorio, R. Saito, J. H. Hafner, C. M. Lieber, M. Hunter, T. McClure, G. Dresselhaus, and M. S. Dresselhaus, Phys. Rev. Lett. **86**, 1118 (2001).
[6] A. G. Souza Filho, S. G. Chou, Ge. G. Samsonidze, G. Dresselhaus, M. S. Dresselhaus, L. An, J. Liu, A. K. Swan, M. S. Ünlü, and B. B. Goldberg, Phys. Rev. B **69**, 115428 (2004).
[7] R. Pfeiffer, H. Kuzmany, C. Schaman, T. Pichler, H. Kataura, Y. Achiba, J. Kürti, and V. Zólyomi, Phys. Rev. Lett. **90**, 225501 (2003).
[8] C. Fantini, A. Jorio, M. Souza, A. J. Mai Jr., M. S. Strano, M. S. Dresselhaus, and M. A. Pimenta, Phys. Rev. Lett. **93**, 147406 (2004).
[9] T. Ono, H. Miyashita, and M. Esashi, Nanotechnology **13**, 62 (2002).
[10] Y. Zhang, A. Chang, J. Cao, Q. Wang,W. Kim, Y. Li, N. Morris, E. Yenilmez, J. Kong, and H. Dai, Appl. Phys. Lett. **79**, 19 (2001).
[11] J. Kong, H. T. Soh, A. M. Casswell, C. F. Quate, and H. Dai, Nature (London) **395**, 878 (1998).
[12] E. Joselevich and C. M. Lieber, Nano Lett. **2**, 10,1137 (2002).
[13] A. Jorio, M. A. Pimenta, A. G. Souza Filho, Ge. G. Samsonidze, A. K. Swan, M. S. Ünlü, B. B. Goldberg, R. Saito, G. Dresselhaus, and M. S. Dresselhaus, Phys. Rev. Lett. **90**, 107403 (2003).
[14] M. S. Dresselhaus, G. Dresselhaus, A. Jorio, A. G. Souza Filho, and R. Saito, Carbon **40**, 2043 (2002).
[15] P. Corio, S. D. M. Brown, A. Marucci, M. A. Pimenta, K. Kneipp, G. Dresselhaus, and M. S. Dresselhaus, Phys. Rev. B **61**, 13202 (2000).
[16] S. D. M. Brown, P. Corio, A. Marucci, M. A. Pimenta, M. S. Dresselhaus, and G. Dresselhaus, Phys. Rev. B **61**, 7734 (2000).
[17] L. Alvarez, A. Righi, T. Guillard, S. Rols, E. Anglaret, D. Laplaze, and J.-L. Sauvajol, Chem. Phys. Lett. **316**, 186 (2000).
[18] C. Fantini, A. Jorio, M. Souza, L. O. Ladeira, M. A. Pimenta, A. G. Souza Filho, R. Saito, Ge. G. Samsonidze, G. Dresselhaus, and M. S. Dresselhaus, Phys. Rev. Lett. **93**, 087401 (2004).
[19] U. J. Kim, X. M. Liu, C. A. Furtado, G. Chen, R. Saito, J. Jiang, M. S. Dresselhaus, and P. C. Eklund (submitted).
[20] A. Grüneis, R. Saito, J. Jiang, Ge. G. Samsonidze, M. A. Pimenta, A. Jorio, A. G. Souza Filho, G. Dresselhaus, and M. S. Dresselhaus, Chem. Phys. Lett. **387**, 301 (2004).
[21] Due to the cutoff of the notch-filter used, the RBM signal is weakened significantly when $\omega_{\mathrm{RBM}} < 220\ \mathrm{cm}^{-1}$, but not when $\omega_{\mathrm{RBM}} > 225\ \mathrm{cm}^{-1}$.